A fuzzy divergence approach for solving electrostatic identification problems for NDT applications

The final publication is available at IOS Press through http://dx.doi.org/ 10.3233/JAE-170043

# A fuzzy divergence approach for solving electrostatic identification problems for NDT applications

Mario Versaci*, Fabio La Foresta, Francesco Carlo Morabito and Giovanni Angiulli
*DICEAM Department, "Mediterranea" University, Via Graziella Feo di Vito, I-89122 Reggio Calabria, Italy*

**Abstract.** This work is devoted to solve the problem of the determination of the spatial position, orientation and size of an electrically charged ellipsoidal conductor subjected to an external electric field. The problem, which is relevant to the field of the non destructive testing and evaluations engineering, is approached in fuzzy domain replacing it in an equivalent classification problem between images through the use of the fuzzy divergence concept. The obtained numerical results demonstrate how the performances of the proposed approach are totally comparable with those given by the more sophisticate and well established fuzzy clustering techniques exploited in literature, offering thus a viable alternative to solve identification problem in electrostatics.

Keywords: Inverse problems, NDT/NDE, fuzzy logic, fuzzy divergences

## 1. Introduction

As is well known, Non Destructive Testing and Evaluation (NDT/NDE) of materials is one of the most important research field within electromagnetics (see [1–3] and references within). In such a context, inverse problems, and in particular the identification ones [4], have been the focus of extensive researches for many years. In the literature, several numerical approaches have been proposed to solve the identification problems at hand with excellent results (see [5–7] and references within). Recently, to estimate condition of existence and uniqueness of this problem, great effort have been made especially from a theoretical point of view. For example, in [8,9] an inverse electrostatic and elasticity problems associated with Poisson and Navier equations were studied for carrying out such conditions. Deterministic and/or nondeterministic methods were applied with inverse and gradient-based inverse problem methodology to identify an electrostatic source using some data monitored along inaccessible boundaries [10]. Furthermore, Finite Element Method (FEM) has been successfully exploited for determining field and potential distributions in order to identify cracks and sources in inaccessible regions [11–14]. However, even if all discussed approaches are characterized by great accuracy, they require both large memory and computational resources sometimes prohibitive especially for real-time applications. In addition,

*Corresponding author: Mario Versaci, DICEAM Department, "Mediterranea" University, Via Graziella Feo di Vito, I-89122 Reggio Calabria, Italy. Tel.: +39 0965 1692273 220 224; E-mail: mario.versaci@unirc.it.

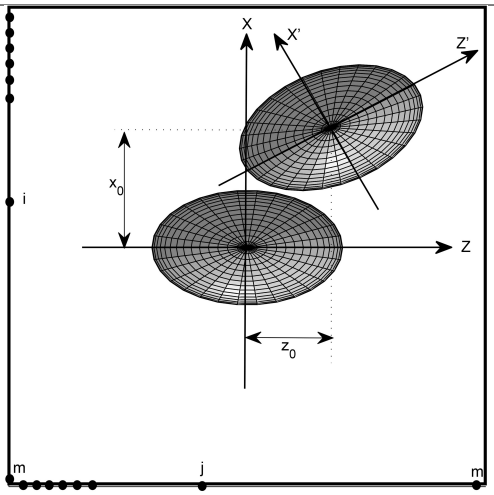


Fig. 1. Ellipsoidal conductor (semi axes $a > b = c$) inside $S^3$: its spatial configuration is uniquely determined by the geometric parameters $z_0$, $x_0$, $\alpha$ and $l$. The dots in bold are the $m$ measuring points of electrostatic potential located along the semi-perimeter of $S^3$.

any uncertainties and/or inaccuracies in the measurements degrade the performance of crisp techniques that do not take into account these eventualities. The advent of soft computing methods, which have been applied with success in many engineering fields (see, for example, [15–18]), allow to overcome these problems. However, since NNs introduce the reader to poorly understand the intimate mechanisms linking input-output pairs, scientific community, for solving identification problems, is increasingly oriented to develop fuzzy applications understandable to non-experts. With this aim, many papers have been published obtaining in order to obtain sophisticated FSs based on banks of fuzzy rules upgradeable by the expert knowledge (see [19] and references within). Although the detection of the defects is considered as a solved problem, the shape reconstruction is still considered as an open problem especially in cases where the defect is not visible and/or not accessible. For example, in the field of civil engineering, the possibility to meet reinforced concrete structural elements in which the metal bars have defectiveness is not negligible. However, the defects found in these structural elements have a shape similar to ellipsoid, and, subjected to certain mechanical loads, such defects are found mostly on particular plans inside the material. So, to solve the identification problem, in these cases, is equivalent to assess the health status of the structural element [20]. In this paper, we propose a novel fuzzy method based on the replacement of a given identification problem at hand into an equivalent problem of fuzzy image classification. In particular, we start from [15] in which multilayer NNs trained via back-propagation procedure was exploited to identify the position, orientation and size of an electrically charged ellipsoidal conductor, located inside an inaccessible area and subjected to an external electric field (see Fig. 1). Our idea is based on the fact that each configuration of the ellipsoid inside the region under study can be considered as an ellipse moving inside a square forbidden area determining a particular distribution of the electrostatic potential measured along the semi-perimeter of the above mentioned area (bold circles in Fig. 1): if the number of sensors is high enough we can construct, for each configuration, a fuzzified image.

Moreover, since similar ellipsoids determine almost superimposed images, they can be grouped into a single class. If for each class an “ad hoc” image is built, the identification of an unknown configuration is reduced to the classification of this unknown image. In the past, the image classification in NDT has been solved by means of fuzzy similarity measurements, in a fuzzy sense, how close an unknown image

is to images characterizing certain classes [21,22]. However, such approaches do not consider the mutual similarity between images so, in this paper, we follow a complementary approach by measuring the total divergence between images taking into account of mutual measurements. In this way the classification is carried out by measuring how far an unknown image is from the representative images of the individual classes. The paper is organized as follows: we start describing the formulation of the identification problem at hand in terms of the position, orientation and size of the charged conducting ellipsoid lying inside the forbidden region under study (Section 2). Later, we describe the proposed procedure of resolution based on the fuzzy divergence concept (Section 3). Numerical results follow (Section 4). In order to validate the performances of the proposed procedure a comparison with those given by the well established soft computing classification techniques such as Fuzzy C-Means Clustering (FCMC) – Fuzzy C-Means Weighted Clustering (FCMWC) – New Fuzzy C-Means Weighted Clustering (NFCMWC) [23] – Simple Fuzzy Similarity Measures (SFSMs) [21,22] is carried out. Finally, some concluding remarks, reported in Section 5, conclude this work.

## 2. Ellipsoidal conductors: An identification problem

This section of the paper is devoted to the description of the problem for determining the geometrical position, orientation and size of an elliptical conductor lying in a forbidden region. In order to obtain the electrostatic potential, the superposition principle is applied. Accordingly, we will give an expression of the total electrostatic potential $V$ easy to implement to obtain the simulated database.

### *2.1. The simulated benchmark*

Let us consider an ellipsoidal conductor charged with a charge $q$ and having semi-axes $a$, $b$ e $c$ (with $a > b = c$) lying in a spatial region denoted with $S^3 \subset \mathbb{R}^3$ filled by a homogeneous isotropic non magnetic linear medium with dielectric permittivity $\epsilon$. If we think $S^3$ as a cube equipped with a system of orthonormal Cartesian axes, $OXYZ$, the analytical expression of the shape of the conductor centered in the origin $O$ and with axes parallel to the coordinate axes, assumes the usual form:

$$f(x, y, z) = \left(\frac{x}{a}\right)^2 + \left(\frac{y}{b}\right)^2 + \left(\frac{z}{c}\right)^2 - 1 = 0. \tag{1}$$

Let us also consider, integral with the conductor, a further system of Cartesian axes $O'X'Y'Z'$ (see Fig. 1). In addition, we suppose that the conductor rototranslates only in the $ZX$ plane ($Y = 0$) for which the system can be considered as an ellipse moving inside the plane $Y = 0$ labeled in the following by $S^2$. Now, the system has now just three degrees of freedom: the coordinates $(z_o, x_o)$ of the center of the conductor and the rotation $\alpha$ around $Y'$ (Fig. 1). On this simulated benchmark, subjected to an external electric field $E_0$, we assume an electrical charge $q$ for which the resulting electrostatic potential $v$ will be formed by overlapping the effects.

### *2.2. Electrostatic potential in a point $P$ external to the forbidden region due to electric charge $q$*

If we consider an ellipsoidal coordinate systems $(\xi, \eta, \zeta)$ ($\xi = 0$ is the ellipsoid surface) the equipo-

tential surfaces are ellipsoids confocal to Eq. (1) and the potential of a point $P$ external to the conductor with coordinate $\xi$ takes the form [15,25]:

$$v(\xi) = \frac{q}{8\pi\epsilon}\int_{\xi}^{\infty}\frac{d\xi}{R_{\xi}} \tag{2}$$

where $R_{\xi} = \sqrt{(a^2+\xi)(b^2+\xi)(c^2+\xi)}$ and the Legendre's integral in Eq. (2) is of the first kind. In our case, as $a > b = c$ the system is of type prolate spheroidal for which $v(\xi)$ in Eq. (2) becomes [15,25]:

$$v(\xi) = \frac{q}{8\pi\epsilon l}\left(\frac{\sqrt{\xi+a^2}+l}{\sqrt{\xi+a^2}-l}\right) = \frac{q}{8\pi\epsilon l} arcth\left(\frac{l}{\sqrt{\xi+a^2}}\right). \tag{3}$$

where $l = \sqrt{a^2-b^2}$ is the focal semi-distance of the shape of the conductor. If $Z$ is the axis of revolution, $\{z, x\}$ represents a system of coordinates of the plane passing through the axis of symmetry, by means of Eq. (3), a generic point $P \in ZX$ outside the conductor takes the following value of potential [15,25]:

$$v(P) = \frac{q}{8\pi\epsilon l}\left[ln\frac{(|z|+l)+\sqrt{x^2+(|z|+l)^2}}{(|z|-l)+\sqrt{x^2+(|z|-l)^2}}\right]. \tag{4}$$

In $S^2$, ideally inaccessible by a "non-transparent" perimeter, it is not possible to see the exact position of the ellipsoid so that we place along the semi perimeter of $S^2$ a set of sensors of potential as showed in Fig. 1. Then, besides the already mentioned parameters of position, it is necessary to consider the geometric parameters $a$ and $b$ constituting, for the purposes of the inverse problem solution, a system in five degrees of freedom.

### *2.3. Electrostatic potential of a point $P$ external to the ellipsoidal conductor due to an external electric field $\vec{E_0}$*

If the region under study is subjected to an external electric field $\vec{E_0} = E_0\hat{i}$ parallel to $X$ axes, the electrostatic potential takes the form $v_0 = -E_0 x$ from which, taking also into account the potential due to the charges induced on the conductor, we obtain the expression:

$$v = v_0\left[1 - \frac{\int_{\xi}^{\infty}\frac{d\xi}{(\xi+a^2)R_{\xi}}}{\int_{0}^{\infty}\frac{d\xi}{(\xi+a^2)R_{\xi}}}\right] \tag{5}$$

where the integrals in Eq. (5) are, according to Legendre's theory, elliptical of the second kind. Obviously, on the surface of the conductor ($\xi = 0$) $v = 0$ while for $\xi \to \infty$, $v \to v_0$. On the other hand, the potential due to the charge distributed on the conductor is obtained by overlapping the effects:

$$v^* = v + \frac{p}{8\pi\epsilon_0 l}\int_{\xi}^{\infty}\frac{d\xi}{R_{\xi}}. \tag{6}$$

In order to build a simulated database of electric potential measurements, along the semi-perimeter of $S^2$ (Fig. 1), the measuring points are computable with the following expression:

$$v = -E_0 x\left\{1 - \left[ln\left(\frac{\sqrt{1+\frac{\xi}{a^2}}+e}{\sqrt{1+\frac{\xi}{a^2}}-e}\right) - \frac{2e}{\sqrt{1+\frac{\xi}{a^2}}}\right]\left[ln\left(\frac{1+e}{1-e}\right) - 2e\right]\right\} \tag{7}$$

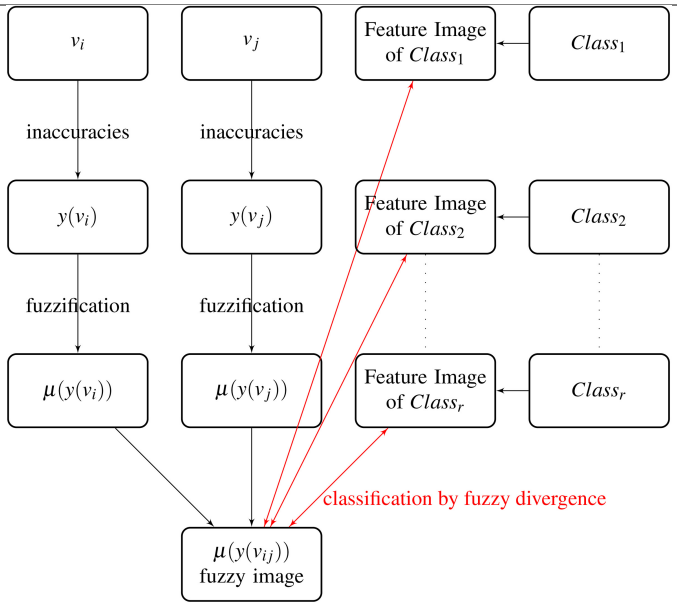


Fig. 2. Flow chart of the proposed approach.

where $e = \sqrt{1-(b/a)^2}$ is the eccentricity of the ellipsoid. The identification problem is to determine the the $4-tuple$, $\{z_0, x_0, \alpha, l\}$, of geometric parameters which determines the distribution of measures, starting from the set of available measures. With this purpose in mind, the authors propose a novel procedure to solve the identification problems replacing it in an equivalent image classification problem, as in the following detailed.

## 3. The proposed approach

### *3.1. A brief overview*

As mentioned in the introduction, the idea of this study is to transform the identification problem in a corresponding image classification problem. The following steps describe the rationale steps (see also the flowchart shown in Fig. 2).

1. Assuming that each ellipsoid configuration determines a distribution of potential values $v$ on the edge of $S^2$ as described in Section 2.2, and if we think of the measurement points ($m$ points for each edge of the semi-perimeter) as a scan of the semi-perimeter, then $S^2$ can be thought as the juxtaposition of $m \times m$ cells, where the generic cell $(i, j)$ is characterized by two values of potential $v_i$, $v_j$ (see Fig. 3).
   Note that $v_i$ is the same value for all cells in the $i$-th row and $v_j$ is the same value for all cells in the $j$-th column and, in addition, $v_i$ and $v_j$ could be different because the potential measured on the edge depends on the distance from the edge of the charge source;
2. Since $v_i$ and $v_j$ simulate realistic measures of potential, we should take into account possible uncertainty and/or imprecision in data. So, at this purpose, we add amounts due to fuzzy inaccuracies to the values obtained by the pseudo-database;

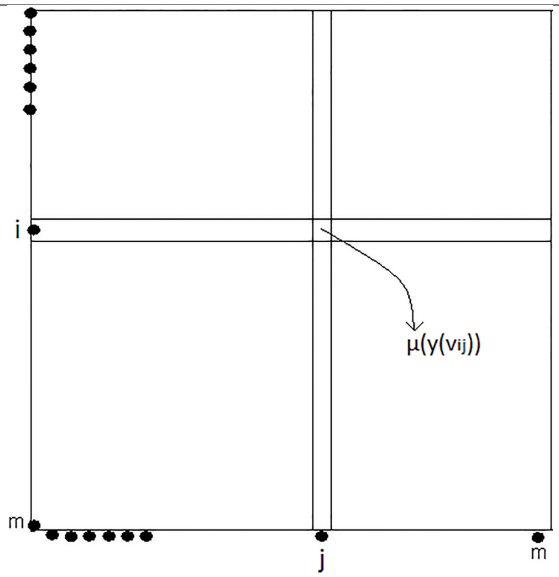


Fig. 3. $2m$ measurements scanned points lying on the boundaries of the forbbiden region determine an $m \times m$ partition of the region $S^3$ : the generic cell $(i, j)$ is characterized by means of two potential values, $v_i$ e $v_j$ which, appropriately weighed, determine the value $v_{ij}$.

3. Indicating by $y(v_i)$ and $y(v_j)$ the potential values included the fuzzy inaccuracies,[1] we denote by $\mu(y(v_i))$ and $\mu(y(v_j))$ the fuzzified values of $v_i$ and $v_j$;
4. A suitable technique of calculation of the amount of the information content will combine $\mu(y(v_i))$ and $\mu(y(v_j))$ in one fuzzified image $\mu(y(v_{ij}))$ (see Fig. 3). So that, for each ellipsoid configuration (in terms of position and size) a fuzzified image $\mu(y(v_{ij}))$ will be carried out;
5. It is observable that ellipsoids close together determine similar images that can be grouped into a single class. For which, starting from a particular configuration of the ellipsoid and varying it slightly, we get a number of fuzzified images of potential distributions equal to the number of the location changes in order to take into account the image obtained from the initial position of the ellipsoid. We will also get a number of classes equal to the number of starting positions of the ellipsoid;
6. in addition regarding the previously classes, it should be consider a further class of images produced by the absence of conductor (containing a single image with $v_{ij} = 0$);
7. treating fuzzy images, we need to evaluate the fuzziness amount contained in each of them. This operation will be carried out through specific indices;
8. since each class is constituted by a certain number of images, by means of appropriate fuzzy image fusion technique, we extract a unique image that representative of the class (feature image);
9. the identification process will take place as follows: an unknown configuration of the ellipsoid determines a pair of distribution of electrostatic potential which, as explained in previous steps, it will be transformed in a single fuzzy image. By computing all of fuzzy divergence values between that image and the feature images of each class, we will get a set of numerical values of fuzzy divergence: the minimum of these values will determine the membership of the unknown configuration to the class generating the minimum value of divergences.

[1] In other words, being $v_i$ a matrix, $y_i = v_i + (\textit{fuzzy inaccuracy})_i$ is still a matrix.

### 3.2. Detailed description

#### 3.2.1. Fuzzy divergence for solving the inverse problem by image classification

In digital image processing, fuzzy logic and procedures are consolidated especially in cases where the presence of uncertainties and/or inaccuracies may affect the applicability of analytical/numerical crisp techniques. Based on fuzzy logic, fuzzy image processing exploits both fuzzy logic and its powerful relational aspects. In this work, both fuzzy divergence and fuzzy image fusion techniques are exploited to solve the inverse problem at hand translating it into an equivalent image classification problem.

#### 3.2.2. Distribution of potential values as fuzzy images

In this work, the distribution of the electrostatic potential $v_i$ of a given configuration of a generic ellipsoidal conductor is conceived as an $m \times m$ image $I$ to which, for each pixel, we associate its gray level $y(v_i)$. Fuzzically, the image $I$, thought as a collection of elements having a certain membership degree, is constituted by an arrangement of $m \times m$ membership values $\mu_I(y(v_i))$, defined on $I$ and ranging on $[0, 1]$, which establish the membership of $y_i$ to $I$ (see Section 3.2.3 for details). If $\mu_I(y(v_i)) = 1$, $y(v_i)$ totally belongs to $I$; if $\mu_I(y(v_i)) = 0$, $y(v_i)$ does not belong to $I$ in a fuzzy sense. If, finally, $\mu_I(y(v_i)) \in (0, 1)$, $y(v_i)$ partially belongs to $I$. Then, an image $I$ can be mathematically defined by:

$$\sum_{i=1}^{m\times m} \{y(v_i),\ \mu_I(y(v_i)),\ \ i = 1, 2, \ldots, m \times m\} \tag{8}$$

where $\sum_{i=1}^{m\times m}$ does not represent a real summation but the juxtaposition of the $m \times m$ pixels arranged in a matrix of $m$ lines and $m$ columns [26]. But, as previously explained, the set of sensors are two (along the semi-perimeter of $S^2$), for each configuration of the simulated benchmark, the formalization Eq. (8) will be doubled: the first one, related to $v_i$, generates the image $I'$; the second one, related to $v_j$, generates the image $I''$. From which, the total amount of information of $\mu_{I'}(y(v_i))$ and $\mu_{I''}(y(v_j))$ will be:

$$\mu_I(y(v_{ij})) = e^{\mu_{I'}(y(v_i))}/e^{\mu_{I''}(y(v_j))} \tag{9}$$

where $I$ represents the resulting image starting from $I'$ and $I''$.

#### 3.2.3. Image fuzzification

Carried out an $m \times m$ image $I$ with $L$ gray-levels starting from a given distribution of electrostatic potential $v_i$ (or $v_j$), as said before, it must be fuzzified. In the literature, there are many image fuzzification procedures [26]. However, with the aim of saving the computational load, the authors propose the use of the following relation [26]:

$$\mu_I(y(v_i)) = \left[1 + \frac{\mathit{max}(y(v_i)) - (y(v_i))}{F_1}\right]^{-F_2}. \tag{10}$$

where $y(v_i)$ is the gray-level of a generic distribution $v_i$, $\mathit{max}(y(v_i))$ and $\mathit{min}(y(v_i))$ are the maximum and minimum of these values respectively and $F_1$ and $F_2$ are the denominational and the exponential fuzzifier coefficients. We proceeds in a similar manner to $v_j$. It is easy to see that $\mu_I(\cdot) \to 1$ when $y(v_i) \to \mathit{max}(y(v_i))$ in such a way that the fuzzified membership degree tends to 1 for cells characterized by higher brilliance.

*3.2.4. Classes construction and constitution of the image feature*

If we consider $n$ very close ellipsoidal conductors (in both position and size), they determine a set of $n$ fuzzified images $I_{1k}, I_{2k} \dots I_{nk}$ of electrostatic potentials almost overlapping each other but grouped in a single class. Let $Class_c$, $c = 1, 2, \dots, k, \dots, r$, be the totality of the classes whose $k$-th class, taking into account the relation Eq. (8), is mathematically representable as follows:

$$\begin{aligned} Class_k = \Big\{ \Big[ \sum_{i=1}^{m} \sum_{j=1}^{m} \{ y(v_{ij}),\ \mu_{I_{1k}}(y(v_{ij})),\ \ i = 1, 2, \dots, m, j = 1, 2, ..., m \} \Big]_k, \\ \Big[ \sum_{i=1}^{m} \sum_{j=1}^{m} \{ y(v_{ij}),\ \mu_{I_{2k}}(y(v_{ij})),\ \ i = 1, 2, \dots, m, j = 1, 2, \dots, m \} \Big]_k, \dots, \\ \dots, \Big[ \sum_{i=1}^{m} \sum_{j=1}^{m} \{ y(v_{ij}),\ \mu_{I_{nk}}(y(v_{ij})),\ \ i = 1, 2, \dots, m, \end{aligned} \tag{11}$$

From the $r$ sets Eq. (11) we will extract $r$ images, $ImageClass_k$, formalized through:

$$ImageClass_k = \Big[ \sum_{i=1}^{m} \sum_{j=1}^{m} \{ y(v_{ij}),\ \sum_{t=1}^{n} \frac{\mu_{I_{tk}}(y(v_{ij}))}{n},\ \ i = 1, 2, \dots, m, j = 1, 2, \dots, m \Big]_k \tag{12}$$

whose membership values are quantified as $\sum_{t=1}^{n} \frac{\mu_{I_{tk}}(y(v_{ij}))}{n}$. So, given a set of $n$ images pertaining to a single class, by Eq. (12), we have obtained a single image $ImageClass_k$, representative of the class (feature image). Ultimately, as the obtained classes are $\widetilde{m}$, we obtain $\widetilde{m}$ feature images. A distribution of electrostatic potential due to a simulated unknown benchmark configuration generates an image $I_{unknown}$ that diverges to varying degrees from $m$ feature images of each class. If

$$\{Div(I_{unknown}, ImageClass_k), k = 1, 2, \dots, \widetilde{m}\}$$

is the set of the fuzzy divergences computed between $I_{unknown}$ and all $ImageClass_k$, and again

$$\{Div(ImageClass_k, I_{unknown}), k = 1, 2, \dots, \widetilde{m}\}$$

is the set of their respective duals, then

$$\{Div(ImageClass_k, I_{unknown}) + Div(I_{unknown}, ImageClass_k), k = 1, 2, \dots, \widetilde{m}\}$$

represents the set of fuzzy total fuzzy divergences between $I_{unknown}$ and all classes. So, the quantity

$$min\{Div(ImageClass_k, I_{unknown}) + Div(I_{unknown}, ImageClass_k), k = 1, 2, \dots, \widetilde{m}\} \tag{13}$$

will determine the membership of $I_{unknown}$ to the class generating such minimum value. In this terms, the inverse problem is transformed into an equivalent image classification problem. The next Section is devoted to a brief overview of the basic concepts that govern the theory of divergence between fuzzy images which will be used below to classify the images. However, before applying any fuzzy technique of image classification, it is good practice to asses the fuzziness contained in each of them by means of specific indexes. In Section 3.2.5 the details of the operational decisions on the basis of goals.

*3.2.5. Fuzziness evaluations by means of specific indexes*

Generally, we define the index of fuzziness of an image $A$, ***IF(A)***, by means of the known relationship [26]:

$$IF(A) = \Big(\frac{2}{n^k}\Big) d(A, \overline{A}) \tag{14}$$

where $d(A, \overline{A})$ denotes the distance between image $A$ and its nearest ordinary image $\overline{A}$ defined by a membership function, $\mu_{\overline{A}}(y(v_{ij}))$ such that $\mu_{\overline{A}}(y(v_{ij})) = 0$ if $\mu_A(x_{ij}) \leqslant 0.5$ and $\mu_{\overline{A}}(x_{ij}) = 1$ if $\mu_A(x_{ij}) > 0$. For our objective, starting from Eq. (14), we exploit the Yager's measure [33] to quantify fuzziness of an image as dependent on the relationship between an image $A$ and its complementary $\overline{A}$. Mathematically, if:

$$D_p(A, \overline{A}) = \Big( \sum_{i}^{m} \sum_{j}^{m} \Big| \mu_A(y(v_{ij})) - \mu_{\overline{A}}(y(v_{ij})) \Big|^{\frac{1}{p}} \Big) \tag{15}$$

represents the distance between $A$ and its complementary, then the Yager's measure, $IF_{Yager}$, is defined as:

$$IF_{Yager} = 1 - \frac{D_p(A, \overline{A})}{|A|^{\frac{1}{p}}} \tag{16}$$

which is particularized in the Hamming distance when $p = 1$ and in the Euclidean one if $p = 2$. $IF_{Yager}$ has been exploited in this work in order to assess the fuzziness amount contained in each image.

*3.2.6. Basics on fuzzy divergences approach*

In order to understand how the Fuzzy Divergence (***FD***) operator between images works, it is necessary to formalize it by means a binary relation over $F(A)$, where $F(A)$ is the universe of the discourse of the grid points of an image $A$ writable in terms of fuzzy distance. Mathematically:

$$FD{:}F(A) \times F(A) \rightarrow [0, \infty] \tag{17}$$

whereby, if $X$ is the universe of discourse, if $F(X)$ is the totality of fuzzy set constructible on $X$ and by $A$ and $B$ we indicate two fuzzy images, then $A, B \in F(X)$. In addition, indicating with $\mu_A(y(v_{ij}))$ and $\mu_B(y(v_{ij}))$ the fuzzified images of $A$ and $B$ respectively, the properties of $FD{:}F(X) \times F(X) \rightarrow [0, \infty]$ between them can be formalized as follows [24,26–29]:

1. $FD(A,B) = FD(B,A), \forall A, B \in F(X)$. In other words, the divergence does not depend on the order with which the fuzzy sets are considered;
2. $\forall A, B, C \in F(X)$, with $A \subset B \subset C$, then $FD(A,B) \leqslant FD(A,C)$ and $FD(B,C) \leqslant FD(A,C)$;
3. $FD(A,A) = 0 \; \forall A \in F(X)$ in the sense that each image $A$ is perfectly comparable to itself;
4. $FD(C, \overline{C}) = max_{A,B \in F(X)} FD(A, B), \forall C \in P(X)$ where $P(X)$ is the totality of the crisp set on $X$ and $\overline{C}$ is the conjugate of $C$.

Starting from [32] where ***FD*** measures was achieved from fuzzy exponential entropy concepts exploiting a single row vector and extending this approach to an image represented by an $m \times m$ with $L$ gray-levels with probabilities $(p_1, p_2, p_3, \ldots, p_L)$, [26]:

$$H(A) = \frac{1}{m^2(\sqrt{e}-1)} \sum_{i=1}^{n}\sum_{j=1}^{n}[(\mu_A(y(v_{ij}))e^{1-\mu_A(y(v_{ij}))+} \\ (1-\mu_A(y(v_{ij})))e^{\mu_A(y(v_{ij}))} - 1] \tag{18}$$

where $y(v_{ij})$ represents the $ij$-th gray-level and $\mu_A(y(v_{ij}))$ represents its fuzzified value. Then if we consider two images, $A$ and $B$, $\forall(i,j)$th pixel, the information of discrimination between $\mu_A(y(v_{ij}))$ and $\mu_A(y(v_{ij}))$, computed by $e^{\mu_A(y(v_{ij}))}/e^{\mu_A(y(v_{ij}))}$, it help us to assess how much the first image diverges form the second one (*Div(A,B)*) and, vice versa, how much the second image diverges from the first one (*Div(B,A)*). Formally:

$$\textit{Div(A,B)} = \sum_{i=1}^{m}\sum_{j=1}^{m}(1-(1-\mu_A(y(v_{ij}))))e^{\mu_A(y(v_{ij}))-\mu_B(y(v_{ij}))} - \\ -\mu_A(y(v_{ij}))e^{\mu_B(y(v_{ij}))-\mu_A(y(v_{ij}))}) \tag{19}$$

$$\textit{Div(B,A)} = \sum_{i=1}^{m}\sum_{j=1}^{m}(1-(1-\mu_B(y(v_{ij})))e^{\mu_B(y(v_{ij}))-\mu_A(y(v_{ij}))} - \\ -\mu_B(y(v_{ij})))e^{\mu_A(y(v_{ij}))-\mu_B(y(v_{ij}))}). \tag{20}$$

Finally, the total divergence ($\textit{Div}_{\textit{total}}(A,B)$) between the two images will be computed as a mere sum of the individual divergences Eqs (19) and (20):

$$\textit{Div}_{\textit{total}(A,B)} = \textit{Div(A,B)} + \textit{Div(B,A)} = \\ = \sum_{i=1}^{m}\sum_{j=1}^{m}(2-(1-\mu_A(y(v_{ij})))+\mu_B(y(v_{ij})))e^{\mu_A(y(v_{ij}))-\mu_B(y(v_{ij}))} - \\ -(1-(1-\mu_B(y(v_{ij}))+\mu_A(y(v_{ij})))e^{\mu_B(y(v_{ij}))-\mu_A(y(v_{ij}))}) \tag{21}$$

If $A$ is the image built by an unknown configuration of the ellipsoid and $B$ represents any one of the $k$, $\textit{ImageClass}_k$, by means of both Eqs (13) and (21), the classification process will be carried out solving thus the identification problem.

## 4. Numerical results

On each side of the semi-perimeter of $S^2$, $m = 100$ measuring point of electric potential were considered (see Fig. 1). In relation Eq. (6) the ranges of the considered parameters are the following: $z_0 \in [-0.2, 0.2]$, $x_0 \in [-0.2, 0.2]$, $\alpha \in [-45°, 45°]$ and $l \in [0.7, 1.2]$ (see [15]). In particular, for the training phase, five starting positions of the conductor have been considered: the first position with the center in $O$ and with axes parallel to the coordinate axes; the other four in the center of each quadrant of the *ZX* plane with lying of the ellipsoid major axis parallel to the bisector of the its quadrant (starting from the North-East quadrant and proceeding counterclockwise). For each of the five start positions ($t = 5$, $\{z_0, x_0, \alpha, l\}$ were varied so as to obtain variations of the electric potential of the same order of magnitude of the changes impressed to the parameters obtaining potential distributions $v_i$ and $v_j$ that, by means of Eq. (6), provide the corresponding potential maps $v_{ij}$. On each map, a fuzzy noise was randomly added to simulate both uncertainty and imprecision. Finally, a sixth class, constituted by a single

Table 1
The exploited data set

| Training data set | | | |
|---|---|---|---|
| Classes | $N^\circ$ Images | Classes | $N^\circ$ Images |
| $Class_1$ | 100 | $Class_3$ | 100 |
| $Class_2$ | 100 | $Class_4$ | 100 |
| $Class_5$ | 100 | $Class_6$ | 1 |
| Testing data set | | | |
| | $N^\circ$ Images | 80 | |

Table 2
$IF_{Yager}$'s ranges of the images belonging to each class: their high values put in evidence high fuzziness

| Class | $IF_{Yager}$ |
|---|---|
| $Class_1$ | $0.80 \div 0.85$ |
| $Class_2$ | $0.77 \div 0.79$ |
| $Class_3$ | $0.76 \div 0.79$ |
| $Class_4$ | $0.76 \div 0.80$ |
| $Class_5$ | $0.75 \div 0.78$ |

Table 3
Fuzzy divergence values for the test case showed in Fig. 5

| | |
|---|---|
| $Div_{total}(Class_1, I_{unknown}) = 0.66$ | $Div_{total}(Class_2, I_{unknown}) = 0.21$ |
| $Div_{total}(Class_3, I_{unknown}) = 0.79$ | $Div_{total}(Class_4, I_{unknown}) = 0.85$ |
| $Div_{total}(Class_5, I_{unknown}) = 0.51$ | $Div_{total}(Class_6, I_{unknown}) = 0.93$ |

image with $v_{ij} = 0$ was considered. With regard to testing, they were considered a reasonable number of images of $v_{ij}$ with known starting positions that, for our purposes, are considered unknowns. Table 1 shows the details of the structure of the data set.

To test the proposed methodology, an ellipsoidal conductor immersed in vacuum ($\epsilon = 8.854187 \cdot 10^{-12}$F/m) was considered and the procedure has been implemented on Intel Core 2 CPU 1.47 GHz using MatLab R2009a. Regarding to both training and testing databases, for each position of the conductor inside $S^2$, the $v_{ij}$ distributions was obtained and fuzzified by means of Eq. (10) where $F_1 = F_2 = 0.5$ producing the images afferent in each class and the test images. For each class the Yager's measure, $IF_{Yager}$ Eq. (16), has been computed whose high values have confirmed the fuzziness content in each of them. In Table 2, for each class, the ranges of normalized $IF_{Yager}$ are reported (please, note that $Class_6$ does not appear because it is formed by a single image with electrostatic potential equal to zero and therefore without fuzziness).

In addition, by means of Eq. (12) the six $ImageClass_k$ that characterize each class have been achieved (see Fig. 4).

A test case is displayed in Fig. 5 where it appears that the fuzzified image, $I_{unknown}$, due to an unknown configuration of the conductor inside $S^2$, has been classified as an image diverging form $Class_i$ with $i \in \{1, 3, 4, 5, 6\}$ and belonging to $Class_2$ (see Table 3). As showed in Table 4, all fuzzified images have been classified successfully with a percentage higher than 99%. These results are entirely comparable with those obtained by applying FCMC, FCMWC and NFCMWC techniques which however require significant effort in terms of CPU-time (see Table 4).

Small considerations about the sensitivity of classification of the results have been made. In particular, the authors have analyzed how small perturbations of the ellipsoidal conductor shape and its position affected the outcomes of the classification procedure. Numerical experiments indicate that the proposed

Table 4
Performance of the proposed procedure compared to classical Fuzzy C-Means techniques

| Technique | Classification (%) | CPU-time (sec.) |
|---|---|---|
| The Proposed Approach | 99.1 | 2.73 |
| FCMC | 99.4 | 3.08 |
| FCMWC | 99.4 | 3.15 |
| NFCMWC | 99.4 | 3.80 |
| SFSMs | 98.91 | 2.70 |

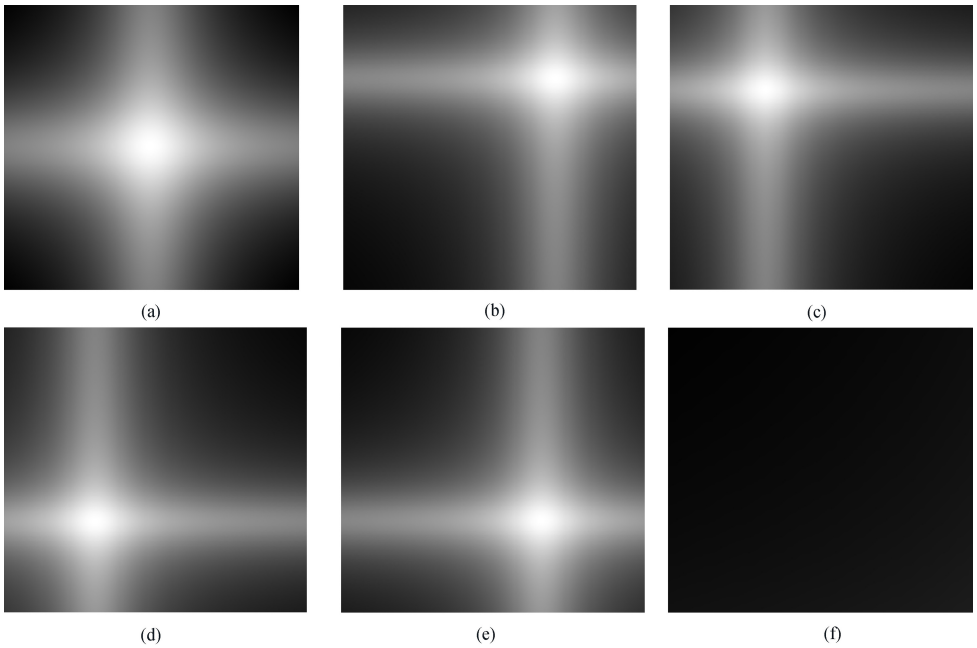


Fig. 4. Features images of each class as described in Section 4: (a) $ImageClass_1$ (b) $ImageClass_2$ (c) $ImageClass_3$ (d) $ImageClass_4$ (e) $ImageClass_5$ and (f) $ImageClass_6$.

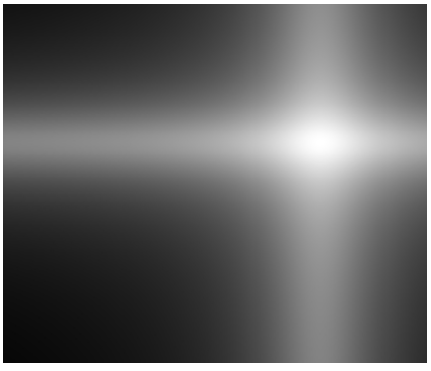

Fig. 5. Test case concerning a configuration of the ellipsoidal conductor classified as belonging to $Class_2$.

procedure is unaffected by perturbations that are smaller than the pixelation of the image. Obviously, the analytical study of the sensitivity will be take into account in future work.

## 5. Summary and concluding remarks

In this paper, a new soft computing approach has been proposed and tested for solving the inverse problem related to the determination of geometric parameters of an electrically charged ellipsoidal conductor subjected to an external field. Starting from a database of simulated measurements generated from the analytical solutions corrupted by an additional fuzzy noise, and building six classes of images of distributions of electrostatic potential generated by known configurations, the identification of an unknown configuration (translated into a fuzzy image) is evaluated by comparison of fuzzy divergence values among images. This procedure, extendibles to many real inverse problems in *NDT/NDE*, has the advantage of solving the problem with an equivalent classification procedure between images characterized by a reduced computational complexity very useful for real-time applications.

## References


[1] F. Yang, Y. Jiang, Q. Shi, T. Chen and W. Wei, Magnetic Field Inverse Problem of Grounding Grid and Its Application, *International Journal of Applied Electromagnetics and Mechanics* **40**(3) (2012), 173–183, doi 103233/JAE-2012-1580.

[2] D. Lahaye, Optimization and Inverse Problems in Electromagnetism, *International Journal of Applied Electromagnetics and Mechanics* **53**(S2) (2017), S1513, doi 103233/JAE-162250.

[3] A. Kharytonov, Solution of Elliptic Inverse Problems using Integral Equations, *International Journal of Applied Electromagnetics and Mechanics* **24**(1-2) (2006), 69–77.

[4] M. Cacciola, Y. Deng, C. Morabito, L. Udpa, S. Udpa and M. Versaci, Automatic Fuzzy Based Identification of Flawed Rivet in Magneto Optic Images, *International Journal of Applied Electromagnetics and Mechanics* **28** (2008), 297–303.

[5] K.R. Aida-zade and A.B. Rahimov, An Approach to Numerical Solution of Some Inverse Problems for Parabolic Equations, *Inverse Problems in Sciences and Engineering* **22**(1) (2004), 96–111, doi 101080/17415997.2013.827184.

[6] S. An, S. Yang, Y. Bai et al., An Improved Physical Programming Method for Multi-Objective Inverse Problems, *International Journal of Applied Electromagnetics and Mechanics* **52**(3-4) (2016), 1151–1159, doi 103233/JAE-162123.

[7] L. Bortolussi, L.P. Dinu, L. Franzoi and A. Sgarro, Coding Theory: A General Framework and Two Inverse Problems, *International Journal of Applied Electromagnetics and Mechanics* **141**(4) (2015), 297–310, doi 103233/FI-2015-1277.

[8] A. Artemev, L. Parnovsky and I. Polterovich, Inverse Electrostatic and Elasticity Problems for Checkered Distributions, *Inverse Problems* **29**(7) (2013), 1–22, doi 101088/0266-5611/29/7/075010.

[9] H. Xiang and J. Zou, Randomized Algorithms for Large-Scale Inverse Problems with General Tikhonov Regularizations, *Inverse Problems* **31**(8) (2015), doi 101088/0266-5611/31/8/085008.

[10] A. Arkadan and S. Subramaniam-Sivanesan, Identifying an Inaccessible Electrostatic Source with Gradient-based Inverse Problem Methodology and Boundary Elements, *IEEE Transactions on Magnetics* **35**(3-Part 1) (1999), 1578–1581.

[11] M. Hadef, M.R. Mekideche, A. Djerdir and A. Miraoui, An inverse problem approach for parameter estimation of interior permanent magnet synchronous motor, *Progress In Electromagnetics Research B* **31** (2011), 15–28, doi 102528/PIERB11021202.

[12] A.A. V.V., Computational Methods for Applied Inverse Problems, in: *Inverse and Ill-Posed Problems*, Y. Wang, A.G. Yagola and C. Yang Eds, Degruyter, Series 56, 2012, ISBN: 978-3-11-025905-6.

[13] S. An, S. Yang and X. Wu, An Improved Multi-Objective Cross-Entropy Method for Inverse Problems, *International Journal of Applied Electromagnetics and Mechanics* **45**(1-4) (2016), 689–695, doi 103233/JAE-141894.

[14] S. Retnajeevan, H. Hoole, S. Subramaniam, R. Saldanha, J.L. Coulomb and J.C. Sabonnadiere, Inverse problem methodology and finite elements in the identification of cracks, sources, materials, and their geometry in inaccessible locations, *IEEE Transactions on Magnetics* **27**(3) (1991), 3433–3443, doi 101109/20.79086.

[15] E. Coccorese, R. Martone and F.C. Morabito, A Neural Network Approach for the Solution of Electric and Magnetic Inverse Problems, *IEEE Transactions on Magnetics* **30**(5) (1994), 2829–2839, doi 101109/20.312527.

[16] G. Angiulli, Design of Square Substrate Integrated Waveguide Cavity Resonators: Compensation of Modelling Errors by Support Vector Regression Machines, *American Journal of Applied Sciences* **9**(11) (2012), 1872–1875, doi 103844/ajassp.2012.1872.

[17] S. Calcagno, F.C. Morabito and M. Versaci, A Novel Approach for Detecting and Classifying Defects in Metallic Plates, *IEEE Transactions on Magnetics* **39**(3) (2003), 1531–1534, doi 101109/TMAG.2003.810353.

[18] M.N. Postorino and M. Versaci, A neuro-fuzzy approach to simulate the user mode choice behaviour in a travel decision framework, *International Journal of Modelling and Simulation* **28**(1) (2008), 64–71.

[19] M. Cacciola, F. La Foresta, F.C. Morabito and M. Versaci, Advanced Use of Soft Computing and Eddy Current Test to Evaluate Mechanical Integrity of Metallic Plates, *NDT & E International* **40** (2007), 357–362, doi 101016/j.ndteint.2006.12.11.

[20] D. Krajcinovic, *Damage Mechanics*, Elsevier Science B.V., Amsterdam, 1996.

[21] D. Pellicanó, I. Palamara, M. Cacciola, S. Calcagno, M. Versaci and F.C. Morabito, Fuzzy Similarity Measures for Detection and Classification of Defects in CFRP, *IEEE Transactions on Ultrasonics, Ferroelectrics, and Frequency Control* **60**(9) (2013), 1917–1927, doi 101109/TUFFC.2013.2776.

[22] M. Versaci, Fuzzy Approach and Eddy Currents NDT/NDE Devices in Industrial Applications, *Electronics Letters* **52**(11) (2016), 943–945, doi 101049/el.2015.3409.

[23] AA.VV., *Fuzzy Sets, Rough Sets, Multisets and Clustering* V. Torra, A. Dahlbom and Y. Narukawa, Editors, Springer International Publishing, doi: 10.1007/978-3-319-47557-8, 2017.

[24] D.G. Wang and Y.P. Meng and H.X. Li, A Fuzzy Similarity Inference Method for Fuzzy Reasoning, *Computers and Mathematics with Applications* **56** (2008), 2445–2454.

[25] L.D. Landau, L.P. Pitaevskii and E.M. Lifsits, *Electrodynamics of Continuous Media* **8**, 2004, Elsevier.

[26] T. Chaira and A.K. Ray, *Fuzzy Image Processing and Application with MatLab*, CRC Press, Taylor & Francis Group, Boca Raton, London New York, 2010.

[27] Z.C. Johaniyak and S. Kovacs, Distance Based Similarities Misures on Fuzzy Sets, in: *Proceedings of the Third Slovakian-Hungarian Joint Symposium on Applied Machine Intelligence*, SAMI 2015, Herl'any, Slovakia (2005).

[28] L. Baccour, A.M. Alimi and R.I. John, Some Notes on Fuzzy Similarity Measures and Application to Classification of Shapes, Recognition of Arabic Sentences and Mosaic, *IAENG International Journal of Computer Science* **41**(2) (2014), 81–90.

[29] D.V. Weken, M. Nachtegael, W.V. De, S. Schulte and E.E. Kerre, A Survey on the Use and the Construction of Fuzzy Similarity Measures in Image Processing, in: *IEEE International Conference on Computational Intelligence for Measurements Systems and Applications*, CIMSA 2005, 2005, pp. 187–192, doi 101109/CIMSA.2005.1522858.

[30] S.K. Pal, R.A. King and A. Hishim, Index of Area Coverage of Fuzzy Image Subset and Object Extraction, *Pattern Recognition Letter* **11** (1992), 831–841.

[31] A. Rosenfeld, The Fuzzy Geometry of Image Subsets, *Pattern Recognition Letter* **2** (1984), 311–317.

[32] J. Fan and W. Xie, Distance Measure and induced Fuzzy Entropy, *Fuzzy Sets and Systems* **104** (1999), 305–314.

[33] R.R. Yager, On the Measure of Fuzziness and Negation I. Membership in Unit Interval, *International Journal of General Systems* **5** (1979), 221–229.

[34] C.C. Hung, S. Kulkarni and B.C. Kuo, A New Weighted Fuzzy C-Means Clustering Algorithm for Remotely Sensed Image Classification, *IEEE Journal of Selected Topics in Signal Processing* **5**(3) (2011), 543–553.